International Journal of Materials Science and Applications
2023; 12(5): 67-74
http://www.sciencepublishinggroup.com/j/ijmsa
doi: 10.11648/j.ijmsa.20231205.12
ISSN: 2327-2635 (Print); ISSN: 2327-2643 (Online)

Study of the Effect of Gallium Replacement by Thallium in $CuGa_{(1-x)}Tl_xS_2$ Structure by First-Principles Calculations on CASTEP

Sangare Kassoum[1, *], Diomande Sékou[1], Bede Affoué Lucie[2]

[1]Department of Agro-Industrial Sciences and Technologies (AIST), UFR Agriculture, Halieutic Resources and Agro-Industry (AHRAI), University of San Pedro, San Pedro, Ivory Coast

[2]Department of Sciences of Structure and Matter (SSMT), Laboratory of Constitution and Reaction of Matter (LCRM), University of Félix Houphouët-Boigny, Abidjan, Ivory Coast

Email address:

kassoum.sangare@usp.edu.ci (Sangare Kassoum), sekou.diomande@usp.edu.ci (Diomande Sékou), lucie.bede@univ-fhb.edu.ci (Bede Affoué Lucie)

[*]Corresponding author

To cite this article:

Sangare Kassoum, Diomande Sékou, Bede Affoué Lucie. Study of the Effect of Gallium Replacement by Thallium in $CuGa_{(1-x)}Tl_xS_2$ Structure by First-Principles Calculations on CASTEP. *International Journal of Materials Science and Applications*. Vol. 12, No. 5, 2023, pp. 67-74. doi: 10.11648/j.ijmsa.20231205.12

Received: September 2, 2023; **Accepted**: September 26, 2023; **Published**: October 14, 2023

Abstract: A natural extension of the zinc-blende compounds from which they crystallographically derive, chalcopyrites are of great interest to the scientific community. Indeed, this family of compounds has many applications, from optoelectronics to diiodes electroluminescence. In order to improve their properties, the current study employs first-principles calculations using the CASTEP software to investigate the effect of gallium substitutional by thallium atoms (Tl_{Ga}) in the $CuGaS_2$ (CGS) chalcopyrite structure. The effect, including structural, electrical and optical properties was studied. Several representatives semiconductors $CuGa_{(1-x)}Tl_xS_2$ were studied, x represents the atomic ratio of Thallium taken from 0 to 40. Properties, convergence of the cutoff energy and the K-mesh were carried out based on first-principles calculations of density functional theory (DFT). The optimized cutoff energy and the optimized K-mesh was found to be 420 eV, 6 6 3 respectively. The results show that, Tl_{Ga} doping induced intermediate band (IB), which can be ascribed to donors' states. That results in a shift of the conduction band minimum (CBM) of CGS towards lower energies. When increasing Tl atomic ratio, the band gap energy decreases from 0.758 (x=0) to 0.172 eV (x=0.40). From optical properties study, $CuGa_{0.78}Tl_{0.22}S_2$, $CuGa_{0.67}Tl_{0.33}S_2$, $CuGa_{0.60}Tl_{0.40}S_2$ showed high absorption coefficient in visible light range, at ca. 1.5 eV. These results suggest that the substitution of Ga by Tl can significantly impact the optical and electrical properties of compounds may have potential applications in photovoltaic, photocatalytic and optoelectronic devices.

Keywords: First-principles Calculations, Doping, Chalcopyrite Structure, Intermediate Band, Band Gap Energy, Absorption Coefficient

1. Introduction

In recent years, a great deal of attention has been paid to chalcopyrite-based ternary semiconductors $A^IB^{III}C_2^{VI}$ where A = Cu, Ag; B = Al, Ga, In; C = S, Se, Te because of their exceptionally tight band gap, high absorption coefficient of ca. 10^4 to 10^6 cm^{-1} [1], good solar stability and excellent chemical stability for corrosion in electrolytes containing water. Such composites demonstrate considerable development potential in a wide range of fields, including photovoltaic cells [2–4], electroluminescent diodes [5, 6] and visible-light photocatalyst [5, 7]. Of these, $CuGaS_2$ is particularly interesting because of its direct band gap by approximately 2.43 eV [8, 9], which makes it suitable for use in photovoltaic (PV), photocatalyst and optoelectronic devices. However, the performance of $CuGaS_2$ can be further enhanced by doping with impurities to tune its electrical and structural properties. Transition and post-transition metal with similar atomic radius

and electronegativity to copper and gallium are suitable for cations doping in CGS [10, 11].

Doping CGS with metals can be achieved by substituting a small amount of copper or gallium with the desired metal ion [11]. The most commonly used metals for dopant are iron [12, 13], cobalt [14], nickel [14], manganese [15, 16], and indium [17–20]. Copper indium gallium di-sulfite (CIGS) is a popular semiconductor material for thin film solar cells, for its high efficiency in converting sunlight into electricity. However, the scarcity and cost of indium and gallium are major issues, which have led researchers to search for alternative materials. Doping CGS creates an intermediate band (IB) within the material's band gap. IB is defined as a band of states which is located in the forbidden band of the semiconducting material. The IB acts as a level for carriers before transitioning for the conduction band (CB) or valence band. Thus, leading to an increase in the efficiency of the devices. Solar cells conversion efficiency depends mainly on its absorbance in the solar spectral region and by the electron hole pair recombination rate. A great approach to get high conversion efficiency is to expand the absorption region of the material by tuning its optical properties [21]. So, the use of thallium, post-transition metal, abundant and less expensive with similar radius to gallium as dopant could affect the band gap energy, the conductivity, and the optical properties of the material. Several works [22-25] have studied the effect of thallium as dopant on the electrical and structural properties of some chalcogenide materials. Mouacher and *al.* [25] have investigated using first-principles codes, the effect of Tl incorporation in Ga sites on $AgGaS_2$ properties. They established that Tl replacement enhances the movement of hole and electron carrier mobility. Tl substitution results in the reduction of bandgap. It also improves the optical properties of $AgGaS_2$ by improving absorption in visible light region.

Current work is performed through a first-principles calculation on CASTEP method to study structural, electrical, and optical properties of $CuGa_{(1-x)}Tl_xS_2$, x is the atomic ratio of Tl. First-principles calculation (simulation) is an essential tool for determining electronic states using quantum mechanics (first principles) as the sole basis to calculate electronic states, without resorting to empirical parameters determined by experiment [26]. The substitution, Tl_{Ga} in the CGS host is expected to have impact on structural, electrical and optical properties of the material, which could make it a promising candidate for use in flexible PV and photocatalyst materials for water splitting.

2. Methodology

The DFT calculations used in this work were carried out on Biovia Materials Studio 2020 using the Cambridge Serial Total Energy Package (CASTEP) under Perdew-Burke-Ernzerhof (PBE) pseudo-potential of the generalized gradient approximation (GGA). The core electrons were treated with the ultrasoft pseudo-potential, and the Kohn-Sham wave functions of the valence electrons. The valence electronic configuration of Cu, Ga, Tl, and S are respectively, Cu: $3d^{10}4s^{1}$, Ga: $3d^{10}4s^{2}4p^{1}$, Tl: $5d^{10}6s^{2}6p^{1}$ and S: $3s^{2}3p^{4}$. In Fine convergence thresholds condition, the convergence parameters were as follows: total energy tolerance 10^{-5} eV/atom, maximum force tolerance 3×10^{-2} eV/Å, and maximum stress component 5×10^{-2} GPa. For precise results, optimized atomic coordinates were obtained by the total energy and atomic forces minimizing. To achieve this, an iterative process was set up, during which the coordinates of the atoms are adjusted so that the total energy of the structure is minimized. By proceeding in this way, we were able to obtain stable structures for all the Tl-doping models. To obtain an accurate cutoff energy and k-mesh, geometry optimization was performed separately on both cells, CGS conventional cell and $CuGa_{(1-x)}Tl_xS_2$ supercell 2×2×2. Based on energy minimization, the cutoff energy of 420 eV was chosen to customize the k-mesh value. From the k-mesh values 2 2 1, 4 4 2, 6 6 3, 8 8 4, the optimal was found to be 6 6 3 for both cells.

3. Results and Discussion

3.1. Structural Properties

The conventional cell and the supercell of Tl-doped $CuGaS_2$ considered in this work are respectively presented in Figure 1 a) and Figure 1 b). The conventional CGS cell has a tetragonal structure (D_{2d}^{13} *space group* $122: I-42bw$) contains four formula units (CGS) per conventional cell. The unit cell contains four copper atoms, four gallium atoms, and eight sulfur atoms. In the tetragonal $CuGaS_2$ crystal structure, each Cu and Ga atom is surrounded by four equivalent S atoms, and each S atom has two equivalent Cu atoms and two equivalent Ga atoms as its nearest neighbors.

After optimization, $CuGaS_2$ conventional cell and supercell have the same lattice parameters and found to be $a = b = 5.351$ Å, $c = 10.48$ Å, $\alpha = \beta = \chi = 90°$. They are in good agreement with experimental and others studies [10, 27, 28]. A change in the chemical composition of $CuGaS_2$ leads to a tetragonal distortion with (2-c/a) different from 0, where a and c are the lattice parameters. The occurring of distortions may be explained by the differences between dopant and doped ion radii and valence electron [29]. In this work, the lattice distortions are not obvious for the Tl-doping structure. This can be explained by Ga and Tl similarly radii and electronegativities [10].

For the supercell, case of thallium doping models, Ga atoms was partially replaced with the Tl impurity. The symmetry was changed to $81: P-4$. Six representatives semiconducting materials in form of $CuGa_{(1-x)}Tl_xS_2$ were studied, *x=0; 0.07; 0.15; 0.22; 0.33; 0.40*. The total formation energy $E_{Tl_{Ga}}$ of these materials are presented in Table 1. The following equation 1 was used [30].

$$E_{Tl_{Ga}} = E_{CuGa_{(1-x)}Tl_xS} + x\mu_{Tl} - (E_{CuGaS_2} + (1-x)\mu_{Ga}) \quad (1)$$

Where $E_{CuGa_{(1-x)}Tl_xS}$ and E_{CuGaS_2} stand for the total energies of the doped and undoped material obtained via CASTEP calculation. The chemical potential $\mu_{Tl} = 1.085236x10^4\ eV$ and $\mu_{Ga} = -1.446705x10^5\ eV$ [25]. All doped materials formation energies are negatives, that shows they are thermodynamically stable. One can see a decrease of

the total formation energy with the increase of Tl concentration. It appears that, based on energy minimization, $CuGa_{(1-x)}Tl_xS_2$ materials are easily formed when increasing dopant concentration.

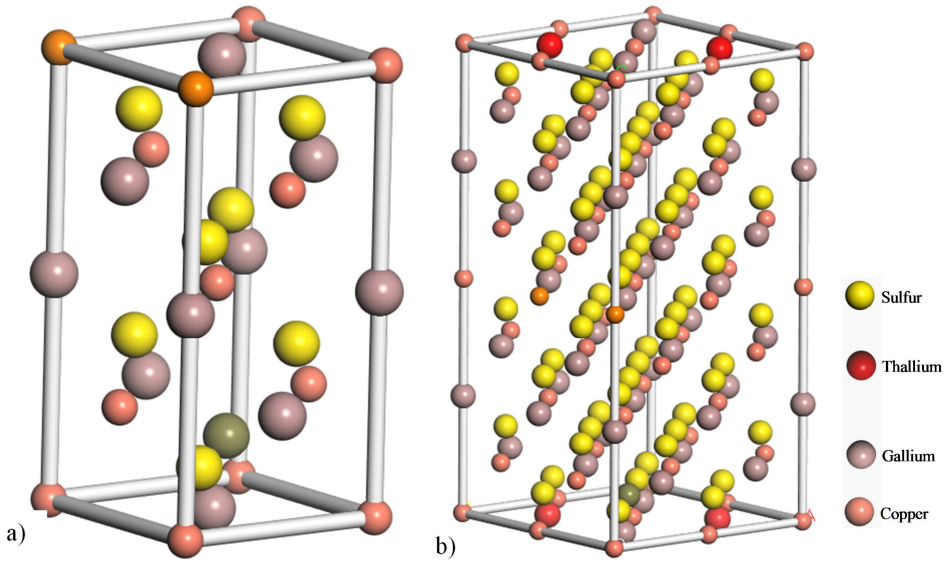

Figure 1. *a) $CuGaS_2$ conventional cell visualization using CASTEP and b) 2×2×2 supercell of typic $CuGa_{0.85}Tl_{0.15}S_2$.*

Table 1. *Calculated total formation energies $E_{Tl_{Ga}}$ of $CuGa_{(1-x)}Tl_xS_2$ materials.*

x (%)	Energy (eV)				
	E_{CuGaS_2}	$E_{CuGa_{(1-x)}Tl_xS}$	μ_{Ga}	μ_{Tl}	$E_{Tl_{Ga}}$
0	-8877.7867	-8877.7868	-144670.5	-10852.4	0
7		-38174.5597			-564569.3329
15		-38174.5601			-1099841.8933
22		-20418.4311			-1617358.3243
33		-20418.4252			-2420267.1584
40		-43499.1706			-2978620.4638

3.2. Electrical Properties

Figure 2 describes the detailed bands structures, the density of state (DOS) and the partial DOS, whereas Figure 3 compare the bands gap energies of CGS and Tl-doped material. All of $CuGa_{(1-x)}Tl_xS_2$ semiconductors have the valence bands maximum and the conduction bands minimum lie along the same symmetry point showing direct band gap semiconductors.

The calculated band gap energies for the five compositions ranges from 0.758 eV to 0.167 eV, showing a decreased of the forbidden band width with the increased of Tl content. The band gap energy calculated are in good agreement with other theoretical studies [31, 32]. Comparing to experimental data [28], the band gap energies of these compounds are underestimated in local-density approximation (LDA) because it doesn't take into account the quasiparticle self-energy correctly [33].

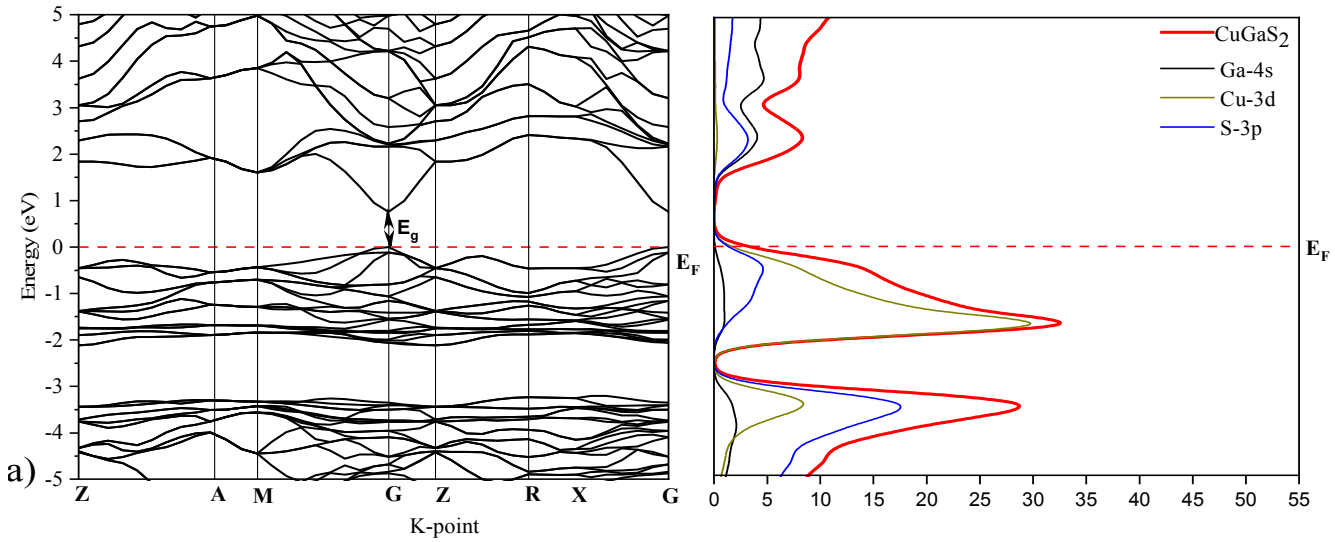

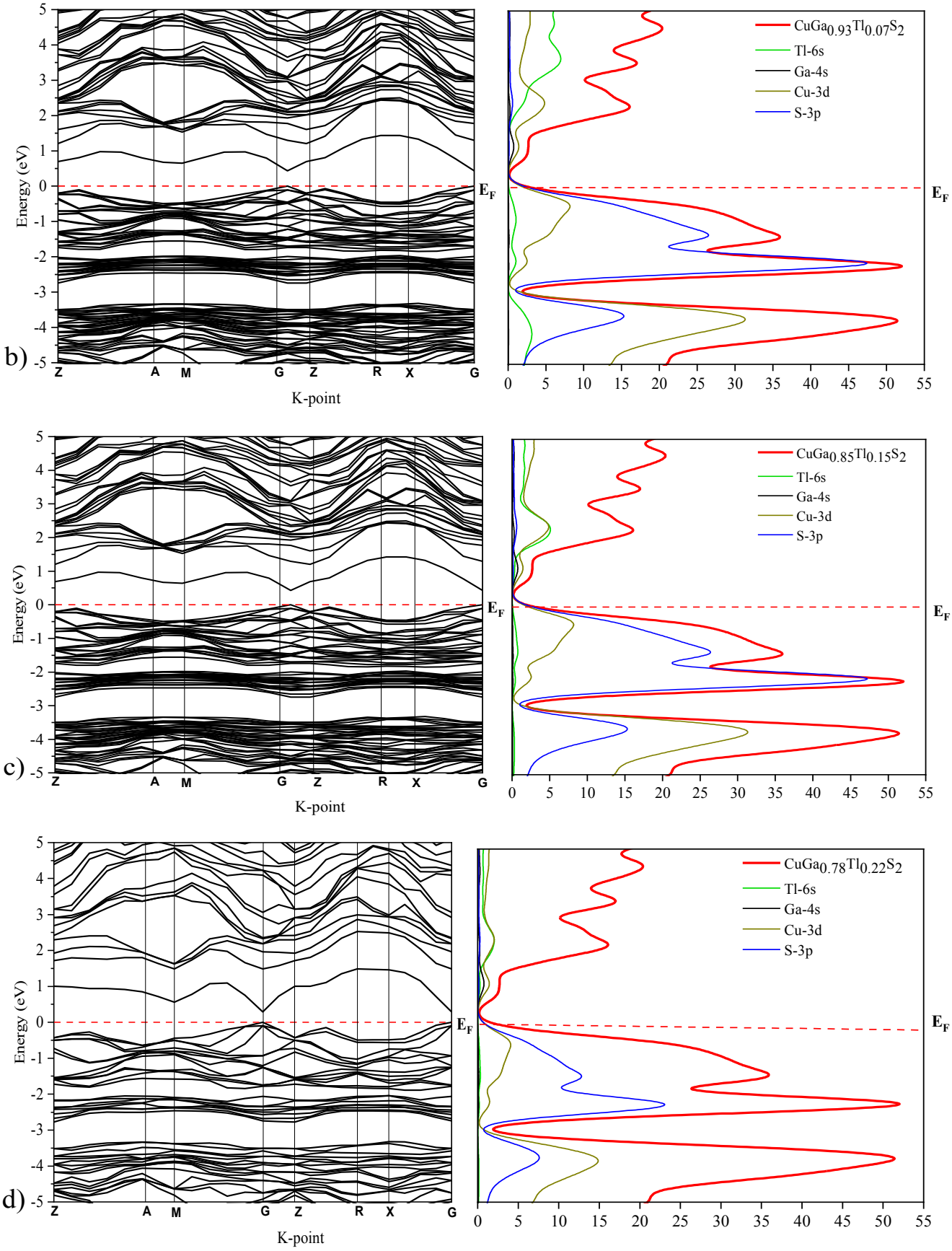
b)
c)
d)
Energy (eV)
K-point
Z
A
M
G
Z
R
X
G
E_F
$CuGa_{0.93}Tl_{0.07}S_2$
$CuGa_{0.85}Tl_{0.15}S_2$
$CuGa_{0.78}Tl_{0.22}S_2$
Tl-6s
Ga-4s
Cu-3d
S-3p

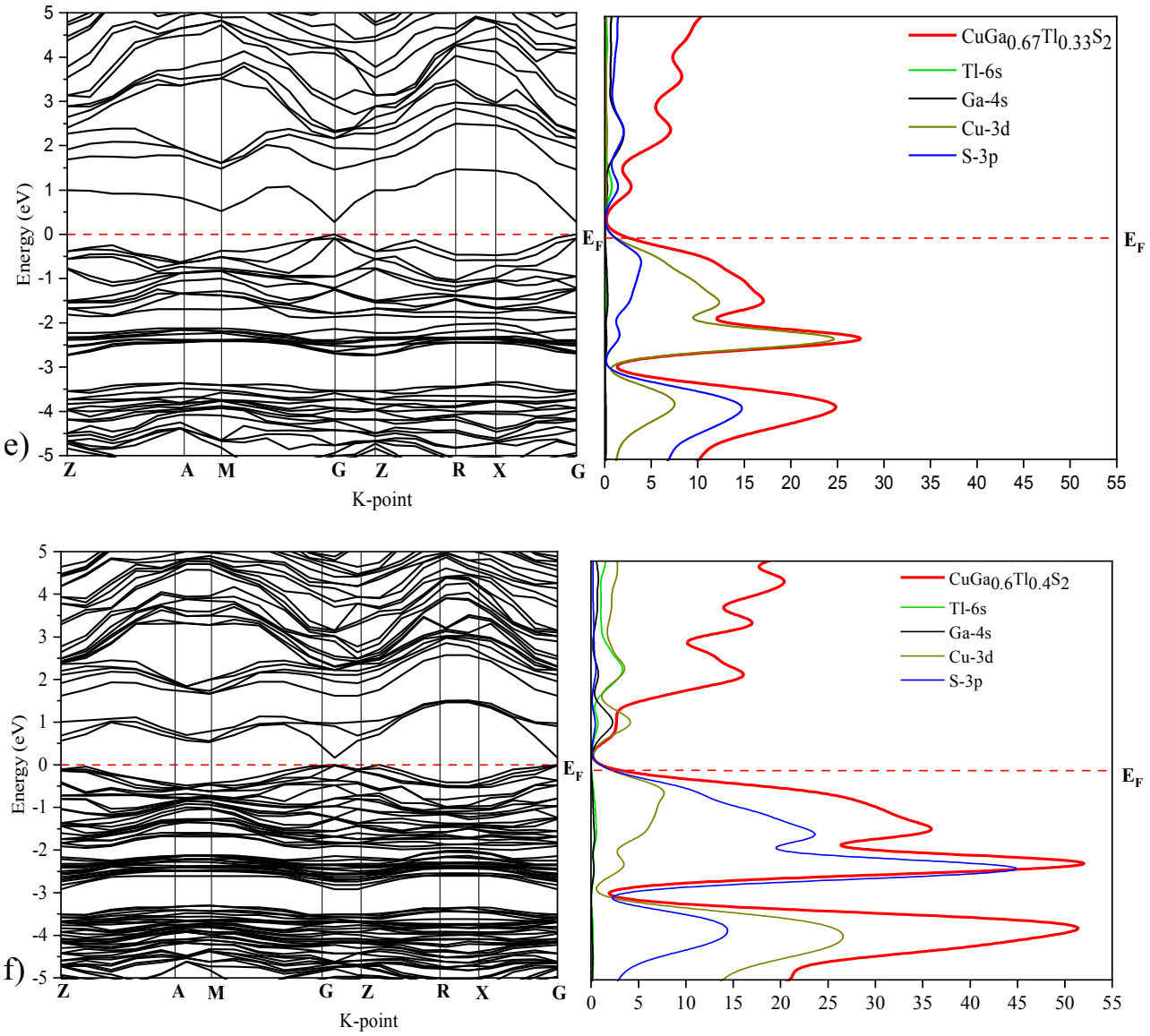

Figure 2. *Bands structures, electrons total and partial density of state (DOS) for a) $CuGaS_2$, b) $CuGa_{0.93}Tl_{0.07}S_2$, c) $CuGa_{0.85}Tl_{0.15}S_2$, d) $CuGa_{0.78}Tl_{0.22}S_2$, e) $CuGa_{0.67}Tl_{0.33}S_2$, f) $CuGa_{0.60}Tl_{0.40}S_2$ calculated using CASTEP code.*

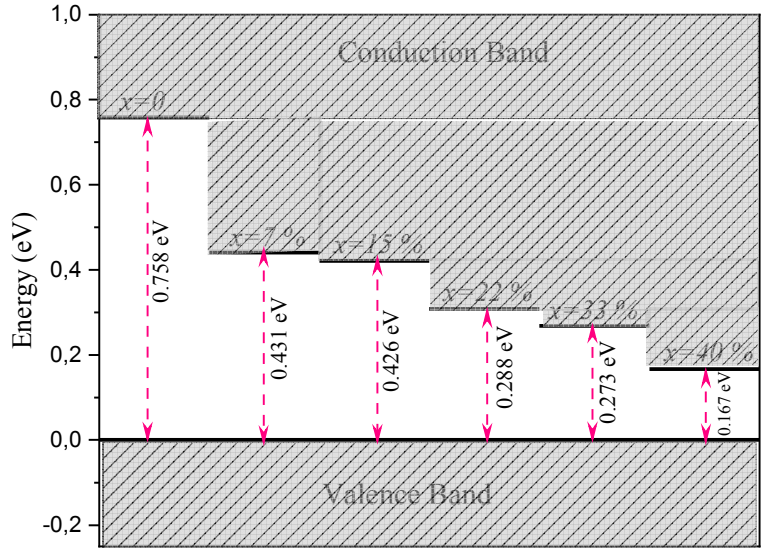

Figure 3. *Comparison of the calculated bands gap energies of $CuGaS_2$ and Tl-doped $CuGaS_2$.*

From partial DOS plot, one can notice that for doped and undoped materials, the valence band (VB) of the materials is split into two parts. Between - 2 eV and 0 eV, the sub-band is essentially composed of both Cu-3d and S-3p states [10, 25]. In more negative energies, we note the contribution of the Ga-4s, Cu-3d and S-3p states. The CB includes both Ga-4s and S-3p states. The hybridization states between S atoms and their neighboring metal atoms consists the electronic states near the bandgap, which dominate the optoelectronic performance [10]. When replacing Ga by Tl atoms, the band structure is essentially modified around the forbidden band without however altering the semiconducting properties of the material. The insertion of Tl atoms, creates in the forbidden band, an intermediate donor band just below the minimum of the conduction band. The new states (IB) are essentially Tl-6s and Ga-4s hybridization states and S-3p [25]. This confirms that the doping is *n*-type and therefore this family of materials can be used as photoanodes in photocatalytic or photovoltaic cells [34].

3.3. Optical Properties

In this study, optoelectronic properties of material are evaluated from absorption coefficient (α) and dielectric function (ε) measurement. Optical parameter analysis provides great information on material response to the electromagnetic spectrum. The dielectric function, $\varepsilon(\omega) = \varepsilon_1(\omega) + i\varepsilon_2(\omega)$, where $\varepsilon_1(\omega)\ and\ \varepsilon_2(\omega)$ represent respectively the real and imaginary part.

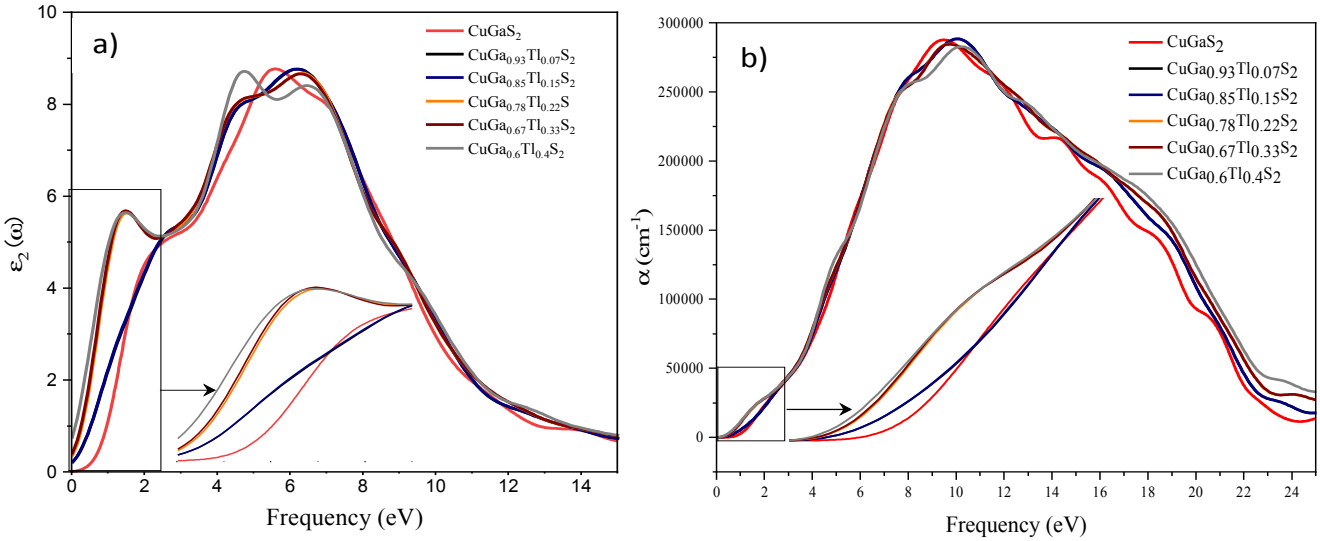

Figure 4. *Comparison of the a) imaginary part of dielectric function (ε₂) spectra and b) the calculated absorption coefficient (α) of $CuGaS_2$ and Tl-doped $CuGaS_2$.*

Figure 4 a) shows imaginary part ($\varepsilon_2(\omega)$) of the dielectric function vs. photon energy (eV) for undoped and Tl-doped materials. From this figure, there is a main peak around 6 eV and a small one at ca. 1.5 eV. For Tl doping materials, the peak appearing in lower energy region is resulting from the absorption of photons due to inter-band transitions between occupied states of valence band and Tl-6s states of intermediate band [35]. The peak is not obvious for Tl contents of 4 and 8%. It can be explained by the small number of available states created by the Tl low doping rate. In Figure 4 b), the absorption coefficient (α) is plot vs. photon energy (eV). For pure CGS, there is a wide absorber peak centered at ca. 9 eV and starting about 2 eV. At about 1.5 eV, the absorption shoulder corresponds to the electron transfer from valence band to the little peak in the conduction band that has very little occupation probability for electrons [10]. Subsequently, the shoulder peak for $CuGa_{0.88}Tl_{0.22}S_2$, $CuGa_{0.67}Tl_{0.33}S_2$ and $CuGa_{0.60}Tl_{0.40}S_2$ have very larger absorption coefficient, more than 10^4 cm^{-1} in visible region. whereas absorption coefficient has no obvious change in the visible-light region for undoped CGS and light doped material, $CuGa_{0.93}Tl_{0.07}S_2$ and $CuGa_{0.85}Tl_{0.15}S_2$. These optical phenomena can be explained clearly from above calculated results about electronic structure, and are in very good agreement with previous study of dielectric imaginary part plot. It is obvious that Tl substitution strongly enhances the absorption coefficient in visible region. These results are in agreement with those of Mouacher *and al*. [25] on the doping of $AgGaS_2$ with thallium.

4. Conclusion

In This work, the impact of the gallium replacement by thallium on the structural, band gap width and optical properties was evaluated. CASTEP calculation shows that, the band gap of $CuGa_{(1-x)}Tl_xS_2$ materials decreases from 0.758 eV to 0.167 eV when Tl-doped rate increased from 0 to 0.40. The decrease in band gap width is the result of the creation of an intermediate band (IB) of donors just below at more negative energy. Analysis of Tl-doped bands structure reveals the

presence of the main hybridization states Tl-6s and S-3p in the (IB). Increasing the Tl rate helps to populate the (IB), which is useful for electronic transitions. From optical properties, it is established that Tl substitution enhances material absorption in visible region. High absorption coefficient was found for high Tl-doping rate, i.e., $CuGa_{0.88}Tl_{0.22}S_2$, $CuGa_{0.67}Tl_{0.33}S_2$ and $CuGa_{0.6}Tl_{0.40}S_2$ makes them suitable for thin film and flexible application, especially as a photoanode in photovoltaic or photocatalytic cells in solar cells.

References

[1] Prabukanthan P, Dhanasekaran R (2007) Growth of $CuGaS_2$ Single Crystals by Chemical Vapor Transport and Characterization. Crystal Growth & Design 7: 618–623. https://doi.org/10.1021/cg060450o

[2] Liu W, Mitzi DB, Yuan M, et al (2010) 12% Efficiency $CuIn(Se,S)_2$ photovoltaic device prepared using a hydrazine solution process. Chemistry of Materials 22: 1010–1014. https://doi.org/10.1021/cm901950q

[3] Akhavan VA, Goodfellow BW, Panthani MG, et al (2010) Spray-deposited $CuInSe_2$ nanocrystal photovoltaics. Energy & Environmental Science 3: 1600–1606. https://doi.org/10.1039/c0ee00098a

[4] Lin YC, Ke JH, Yen WT, et al (2011) Preparation and characterization of $Cu(In,Ga)(Se,S)_2$ films without selenization by co-sputtering from $Cu(In,Ga)Se_2$ quaternary and In 2 S 3 targets. Applied Surface Science 257: 4278–4284. https://doi.org/10.1016/j.apsusc.2010.12.036

[5] Honda T, Hara K, Yoshino J, Kukimoto H (2003) Emission characteristics of $CuGaS_2$-based light-emitting diode grown by metalorganic vapor phase epitaxy. Journal of Physics and Chemistry of Solids 64: 2001–2003. https://doi.org/https://doi.org/10.1016/S0022-3697(03)00254-3

[6] Jaffe JE, Zunger A (1983) Electronic structure of the ternary chalcopyrite semiconductors $CuAlS_2$, $CuGaS_2$, $CuInS_2$, Se_2, $CuGaSe_2$, and $CuInSe_2$. Physical Review B 28: 5822–5847. https://doi.org/10.1103/PhysRevB.28.5822

[7] Leisch JE, Bhattacharya RN, Teeter G, Turner JA (2004) Preparation and characterization of $Cu(In,Ga)(Se,S)_2$ thin films from electrodeposited precursors for hydrogen production. Solar Energy Materials and Solar Cells 81: 249–259. https://doi.org/10.1016/j.solmat.2003.11.006

[8] Lv X, Yang S, Li M, et al (2014) Investigation of a novel intermediate band photovoltaic material with wide spectrum solar absorption based on Ti-substituted $CuGaS_2$. Solar Energy 103: 480–487. https://doi.org/http://dx.doi.org/10.1016/j.solener.2014.02.046

[9] Castellanos Aguila JE, Palacios P, Conesa JC, et al (2016) Electronic band alignment at $CuGaS_2$ chalcopyrite interfaces. Computational Materials Science 121: 79–85. https://doi.org/10.1016/j.commatsci.2016.04.032

[10] Zhao Z, Zhou D, Yi J (2014) Analysis of the electronic structures of 3d transition metals doped $CuGaS_2$ based on DFT calculations. Journal of Semiconductors 35: 13002

[11] Priyadarshini P, Das S, Naik R (2022) A review on metal-doped chalcogenide films and their effect on various optoelectronic properties for different applications. RSC Advances 12: 9599–9620. https://doi.org/10.1039/d2ra00771a

[12] Marsen B, Klemz S, Unold T, Schock H-W (2012) Investigation of the Sub-Bandgap Photoresponse in $CuGaS_2$: Fe for Intermediate Band Solar Cells. Progress in Photovoltaics: Research and Applications 20: 625–629. https://doi.org/https://doi.org/10.1002/pip.1197

[13] Viveka SS, Logu T, Ahsan N, et al (2021) Fe-doped $CuGaS_2$ ($CuGa_{1-x}Fe_xS_2$) - Detailed analysis of the intermediate band optical response of chalcopyrite thin films based on first principle calculations and experimental studies. Materials Science in Semiconductor Processing 136: 106133. https://doi.org/https://doi.org/10.1016/j.mssp.2021.106133

[14] Palacios P, Aguilera I, Wahnón P, Conesa JC (2008) Thermodynamics of the Formation of Ti- and Cr-doped $CuGaS_2$ Intermediate-band Photovoltaic Materials. The Journal of Physical Chemistry C 112: 9525–9529. https://doi.org/10.1021/jp0774185

[15] Picozzi S, Zhao Y-J, Freeman AJ, Delley B (2002) Mn-doped $CuGaS_2$ chalcopyrites: An ab initio study of ferromagnetic semiconductors. Physical Review B 66: 205206. https://doi.org/10.1103/PhysRevB.66.205206

[16] Karwasara H, Khan K, Gaur A, et al (2023) Optoelectronic Analysis of $CuGaS_2$-Based Flexible Thin Film Solar Cell: First Principle Investigation BT - Flexible Electronics for Electric Vehicles. In: Dwivedi S, Singh S, Tiwari M, Shrivastava A (eds). Springer Nature Singapore, Singapore, pp 547–552.

[17] Ramanujam J, Singh UP (2017) Copper indium gallium selenide based solar cells – a review. Energy & Environmental Science 10: 1306–1319. https://doi.org/10.1039/C7EE00826K

[18] Chadel M, Chadel A, Benyoucef B, Aillerie M (2023) Enhancement in Efficiency of CIGS Solar Cell by Using a p-Si BSF Layer. Energies 16.

[19] Kuk S, Wang Z, Jia Z, et al (2019) Effect of Nanosecond Laser Beam Shaping on $Cu(In,Ga)Se_2$ Thin Film Solar Cell Scribing. ACS Appl Energy Mater 2: 5057.

[20] Jeong S, Ham SS, Choi EP, et al (2023) Enhanced Mechanical Stability of CIGS Solar Module with Glass/Polyimide/Indium Tin Oxide for Potentially Flexible Applications. ACS Applied Energy Materials 6: 3745–3755. https://doi.org/10.1021/acsaem.2c03957

[21] Luque A, Martí A (1997) Increasing the Efficiency of Ideal Solar Cells by Photon Induced Transitions at Intermediate Levels. Physical Review Letters 78: 5014–5017. https://doi.org/10.1103/PhysRevLett.78.5014

[22] S A Nemov, Yu I Ravich (1998) Thallium dopant in lead chalcogenides: investigation methods and peculiarities. Physics-Uspekhi 41: 735. https://doi.org/10.1070/PU1998v041n08ABEH000427

[23] Yan B, Liu C-X, Zhang H-J, et al (2010) Theoretical prediction of topological insulators in thallium-based III-V-VI2 ternary chalcogenides. Europhysics Letters 90: 37002. https://doi.org/10.1209/0295-5075/90/37002

[24] Sujith CP, Joseph S, Mathew T, Mathew V (2022) Ab initio investigation of the structural and electronic properties of tantalum thallium chalcogenides $TaTlX_3$ (X = S,Se). Journal of Solid State Chemistry 315: 123534. https://doi.org/https://doi.org/10.1016/j.jssc.2022.123534

[25] Mouacher R, Seddik T, Rezini B, et al (2022) First-principles calculations of electronic and optical properties of $AgGa_{1-x}Tl_xS_2$ alloys: Analyses and design for solar cell applications. Journal of Solid State Chemistry 309: 122996. https://doi.org/https://doi.org/10.1016/j.jssc.2022.122996

[26] Suwa Y, Okamoto M (2014) First-principles Materials-simulation Technology. Hitachi Review 63: 592.

[27] Romero AH, Cardona M, Kremer RK, et al (2011) Electronic and phononic properties of the chalcopyrite $CuGaS_2$. Physical Review B 83: 195208. https://doi.org/10.1103/PhysRevB.83.195208

[28] Sangaré K, Cherfouh H, Marsan B (2021) Synthesis and Characterization of N-Type $CuGaS_2$ Nanoparticles and Films for Purpose of Photoelectrocatalytic Water Splitting. Journal of The Electrochemical Society 168: 86506. https://doi.org/10.1149/1945-7111/ac1cc6

[29] Kokta M, Carruthers JR, Grasso M, et al (1976) Ternary phase relations in the vicinity of chalcopyrite copper gallium sulfide. Journal of Electronic Materials 5: 69–89. https://doi.org/10.1007/BF02652887

[30] Van de Walle CG, Neugebauer J (2004) First-principles calculations for defects and impurities: Applications to III-nitrides. Journal of Applied Physics 95: 3851–3879. https://doi.org/10.1063/1.1682673

[31] Rashkeev SN, Lambrecht WRL (2001) Second-harmonic generation of I-III-VI 2 chalcopyrite semiconductors: Effects of chemical substitutions. Physical Review B 63: 165212.

[32] Laksari S, Chahed A, Abbouni N, et al (2006) First-principles calculations of the structural, electronic and optical properties of $CuGaS_2$ and $AgGaS_2$. Computational materials science 38: 223–230.

[33] Bechstedt F, Del Sole R (1988) Analytical treatment of band-gap underestimates in the local-density approximation. Physical Review B 38: 7710.

[34] Tang R, Zhou S, Zhang Z, et al (2021) Engineering nanostructure–interface of photoanode materials toward photoelectrochemical water oxidation. Advanced Materials 33: 2005389.

[35] Mishra S, Ganguli B (2015) Effect of Na substitution on electronic and optical properties of $CuInS_2$ chalcopyrite semiconductor. Journal of Solid State Chemistry 232: 131–137.